Supporting Information

An $Eu_4L^4_4$ Tetrahedron with multi-recognition sites: A luminescent sensor with rapid and sensitive detection of biogenic amines

Yuan Yao[a], Li Li[a], Tongxi Zhou[a], Su Wang[a], Ying Qin[a], Chao Fan[a], Yuying Fu[a], Guoliang Liu[a*] and Hongfeng Li[b*]

[a*]*College of Sports Science and Health, College of sports science research, Harbin sport university, Harbin 150008, Heilongjiang, People's Republic of China.*

[b*]School of Chemistry and Materials Science, Key Laboratory of Functional Inorganic Material Chemistry, Ministry of Education Heilongjiang University 74 Xuefu Road, Harbin 150080, China.

1. Materials and methods

1.1 Materials and instruments

In this paper all reagents were obtained from the best known commercial sources and used without further purification. ^{1}H NMR spectra were acquired on a Bruker AV 400 spectrometer. Electrospray ionization time-of-flight (ESI-TOF) mass spectra and Electron ionization (EI) spectra were mesured on Bruker maXis mass and Agilent 5973 N spectrometers, respectively. FT-IR spectra of samples were obtained from KBr disks on a Perkin Elmer Spectrum One spectrophotometer. Elemental analyses were performed on an Elementar Vario EL cube analyser. UV-Vis spectra were collected on a Perkin Elmer Lambda 25 spectrometer. Excitation and emission spectra were recorded on an Edinburgh FLS 1000 fluorescence spectrophotometer.

1.2 Synthetic procedures

3, 3', 3 "-trimethoxytriphenylamine (TTA)

m-aminoanisole (1.85 g, 15.00 mmol) and 3-iodoanisole (8.07 g, 34.50 mmol) were dissolved in 100 mL dichlorobenzene. Copper powder (9.45g, 150.00 mmol), 18-crown-6 (2.38 g, 0.90 mmol) and K_2CO_3 (31.16 g, 22.58 mmol) were added to the above solution under nitrogen protection. The reflux reaction was heated for 24 hours, at which point TLC analysis indicated completion. The catalysts were removed by filtration, and the filtrate was washed with dilute ammonia until colorless, followed by several washes with water. The solution was dried over anhydrous sodium sulfate, and excess solvent was removed by rotary evaporation under reduced pressure. A yellow oily liquid (4.11 g, 80.52% yield) was obtained and characterized by thin-layer chromatography (TLC; silica gel, petroleum ether/EtOAc 4:1). ^{1}H NMR (400 MHz, $CDCl_3$): δ 3.73 (m, 9H), 6.57 (m, 3H), 6.66 (m, 6H), 7.16 (t, 3H). HRMS (m/z) (ES+) Calculated for $C_{21}H_{21}NO_3$ m/z = 335.4035 [M]. Found m/z = 335.4083.

3,3',3"-trihydroxy-4, 4', 4" -triacetyl triphenylamine (TTTA)

Acetyl chloride (3.15 g, 40.10 mmol) was added slowly to aqueous aluminum chloride (5.35 g, 40.10 mmol) in 20 mL CH_2Cl_2 and stirred for 30 min. The solution was added dropwise to 1, 2-dichloroethane solution of **TTA** (6.68 g, 2.24 mmol) at 0 °C and stirred for 24 hours at room temperature. The resulting mixture was poured into ice water and filtered to remove the catalysts. The organic phase was separated, washed twice with water, dried over anhydrous Na_2SO_4, and evaporated to dryness. The crude product was recrystallized from acetonitrile to afford yellow needle-like crystals (2.50 g, 81.52% yield). ^{1}H NMR (400 MHz, $CDCl_3$): δ 2.60 (m, 9H), 6.64 (m, 6H), 7.64 (d, 3H), 12.48 (s, 3H). HRMS (m/z) (ES+) Calculated for $C_{24}H_{22}NO_6$ m/z = 420.4421 $[M + H]^+$. Found m/z = 420.4410.

Tri (3- (2-) pyridyl methoxy) - tri (4- : acetyl) triphenylamine (TPTA)

TTTA (0.52 g, 1.25 mmol) and anhydrous K_2CO_3 (2.07 g, 15.00 mmol) were dissolved in 50 mL anhydrous acetone. Then, 2-chloromethyl pyridine hydrochloride (1.22 g, 7.50 mmol) and anhydrous K_2CO_3 (2.07 g, 15.00 mmol) was stirred for 30 minutes at room temperature under nitrogen, then they were added to the above solution and heated for 36 hours, by which time TLC analysis indicated the reaction was complete. After the reaction was completed, the precipitate was filtered, and the filtered solution was concentrated under reduced pressure. It was then poured into the water when brown solid was formed, which was then filtered and the residue was charged by thin-layer chromatography (silica gel, petroleum ether–EtOAc, 1 : 4) to provide the desired product as a yellow powder (0.52 g, 60.03 %). ^{1} H NMR (400 MHz, $CDCl_3$): δ 2.68 (s, 9H), 5.07 (s, 6H), 6.56 (m, 6H), 7.21 (m, 3H), 7.47 (d, 3H), 7.63 (d, 3H), 7.71 (m, 3H), 8.45 (d, 3H). HRMS (m/z) (ES+) Calculated for $C_{42}H_{37}N_4O_6$ m/z = 693.7802 $[M + H]^+$. Found m/z = 693.7810.

(2, 2', 2'')-1,1',1''-(nitrilotris (2-(pyridin-2-ylmethoxy) benzene-4,1-diyl)) tris (4,4,4-trifluoro-3-hydroxybut-2-en-1-one) (L^4)

In 50 mL of ethylene glycol dimethyl ether (DME), ethyl trifluoroacetate (2.30 g, 16.20 mmol) and sodium methoxide (0.87 g, 16.20 mmol) were dissolved and stirred for 30 min at room temperature. **TPTA** (1.87 g, 2.70 mmol) was added and stirred for overnight. The resulting solution was quenched with water and acidified to pH 4–5 using a 2.0 M solution of succinic acid. The yellow precipitate that formed was collected by filtration and dried under vacuum. Recrystallization from acetonitrile afforded yellow needle-like crystals. (2.00 g, 75.61 %). ^{1}H NMR (400 MHz, $CDCl_3$): δ 5.09 (m, 6H), 6.69 (s, 3H), 6.72 (d, 3H), 7.12 (s, 3H), 7.23 (m, 3H), 7.49 (d, 3H), 7.73 (t, 3H), 7.91 (d, 3H), 8.48 (d, 3H), 15.31 (s, 3H). HRMS (m/z) (ES+) Calculated for $C_{48}H_{32}F_9N_4O_9$ m/z = 979.7893 $[M - H]^-$. Found m/z = 979.7820.

Synthesis of $Ln_4L^4_4$ [Ln = Eu, Gd, La]

Triethylamine (0.15 g, 1.50 mmol) and **L^4** (0.49 g, 0.50 mmol) were dissolved completely under stirring in methanol. $LnCl_3{\cdot}6H_2O$ (Ln = Eu, La and Gd; 0.50 mmol) was dissolved in 1 mL methanol, then added to above-mentioned solution and stirred overnight at room temperature. The solution was poured into water and stirred until a yellow precipitate was completely formed. The product was filtered, washed with water (3 × 30 mL), dichloromethane (3 × 30 mL), and n-hexane (3 × 30 mL), and then dried under vacuum.

$Eu_4\mathbf{L^4}_4$. (0.49 g, 87.10%). HRMS (m/z) (ES+) Calculated for $C_{192}H_{120}Eu_4F_{36}N_{16}NaO_{36}$ m/z = 4541.4248 $[M + Na]^+$. Found m/z = 4541.4255; Anal. Calc. For $C_{192}H_{120}Eu_4F_{36}N_{16}O_{36}$: C, 49.45; H, 2.94; N, 4.81. Found: C, 49.12; H, 2.87; N 4.88.

$Gd_4\mathbf{L^4}_4$. (0.50 g, 88.41%). HRMS (m/z) (ES+) Calculated for $C_{192}H_{121}F_{36}Gd_4N_{16}O_{36}$ m/z = 4540.4541 $[M + H]^+$. Found m/z = 4540.4537; Anal. Calc. For $C_{192}H_{120}F_{36}Gd_4N_{16}O_{36}$: C, 49.23; H, 2.93; N, 4.78. Found: C, 49.17; H, 2.97; N, 4.75.

$La_4\mathbf{L^4}_4$. (0.49 g, 87.62%). HRMS (m/z) (ES+) Calculated for $C_{192}H_{121}F_{36}La_4N_{16}O_{36}$ m/z = 4467.3887 $[M + H]^+$. Found m/z = 4467.3892; Anal. Calc. For $C_{192}H_{120}F_{36}La_4N_{16}O_{36}$: C, 50.02; H, 2.97; N, 4.86. Found: C, 49.96; H, 3.05; N, 4.92.

1.3 Test procedures

0.0045 g (10^{-6} mol) was dissolve in 0.5 mL of THF-*d8* (c = 2 × 10^{-3} M), and then record the ^{1}H NMR spectrum of the solution. To the above solution, add putrescine (DAB) in batches, 0.0011 g (12 X 10^{-6} mol)、0.0011 g and 0.0022 g (24 X 10^{-6} mol) each time, for a total of three additions. After each addition, measure the ^{1}H NMR spectrum of the solution. Finally, compare and analyze the four obtained spectra to generate Figure 6.

2. Supplementary Figures and Tables

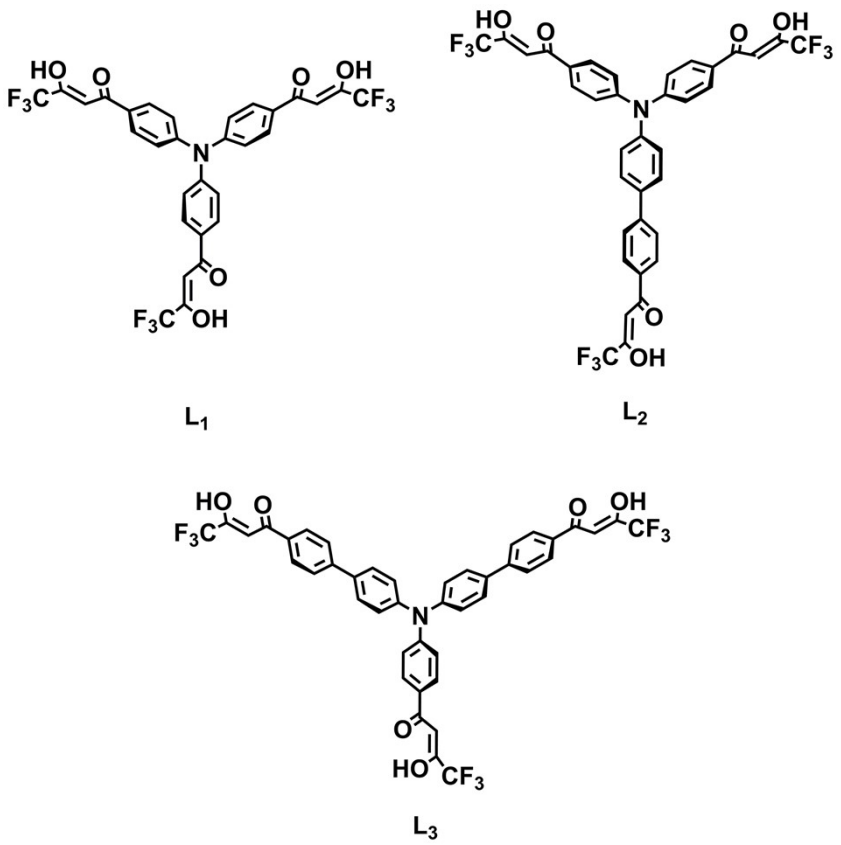

Figure S1 The structures of ligands L^1, L^2 and L^3.

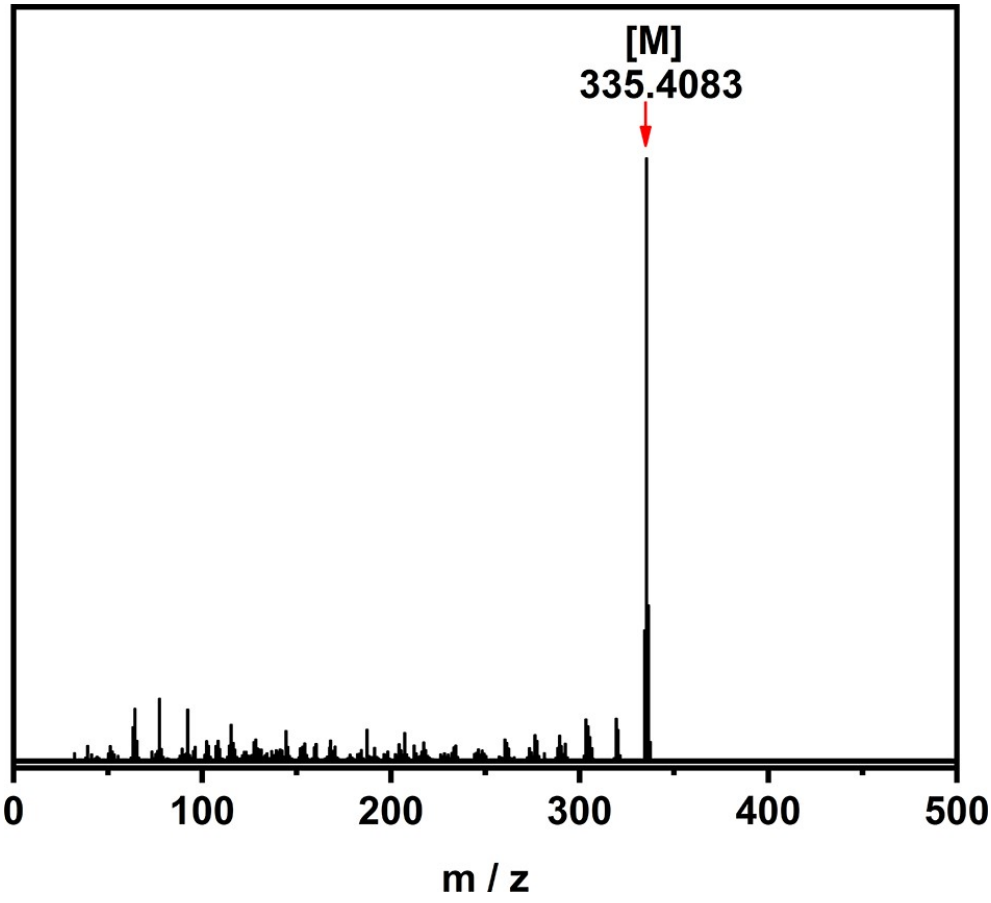

Figure S2 EI-MS spectrum of 3, 3', 3 "-trimethoxy triphenylamine.

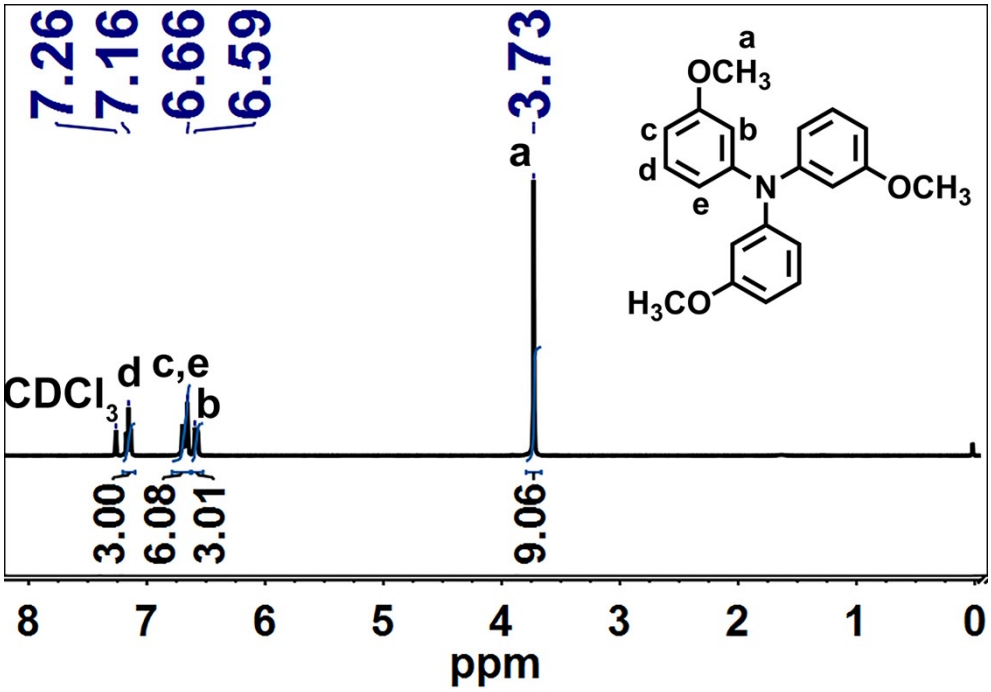

Figure S3 400 MHz ^{1}H NMR spectrum of 3, 3', 3 "-trimethoxy triphenylamine in $CDCl_3$.

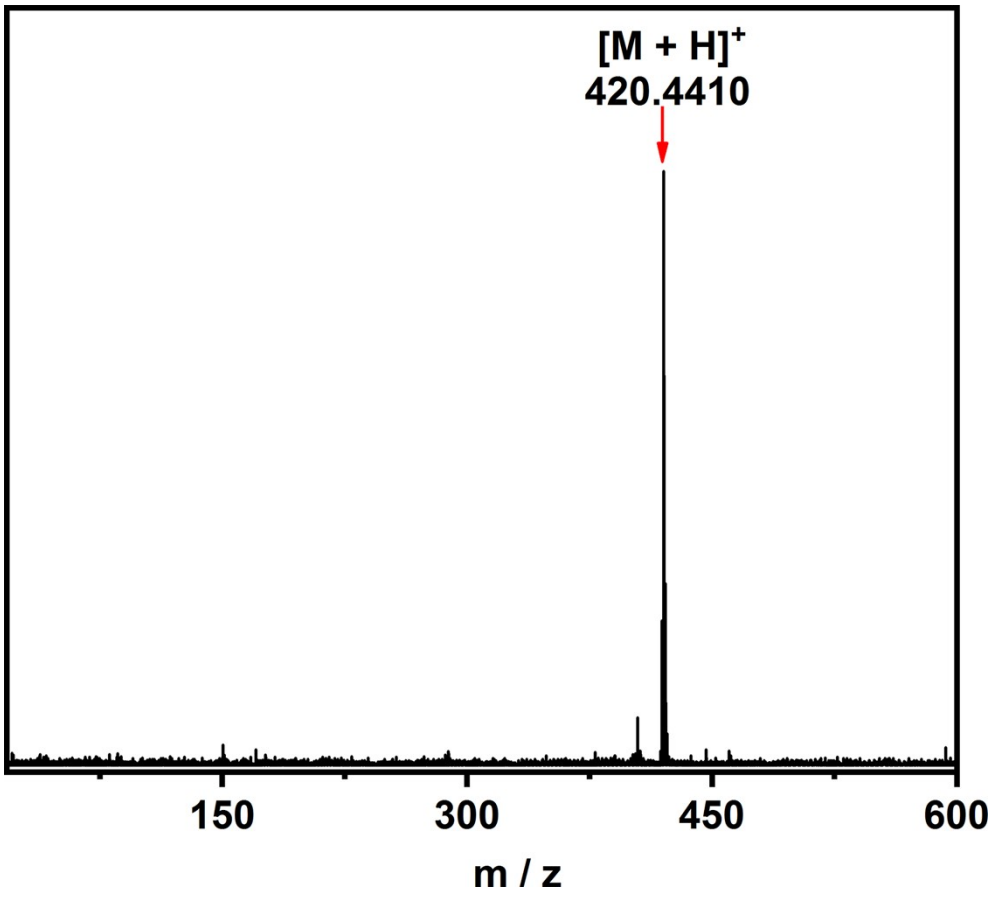

Figure S4 ESI-MS spectrum of 3, 3', 3 "-trihydroxy-4, 4', 4" -triacetyl triphenylamine.

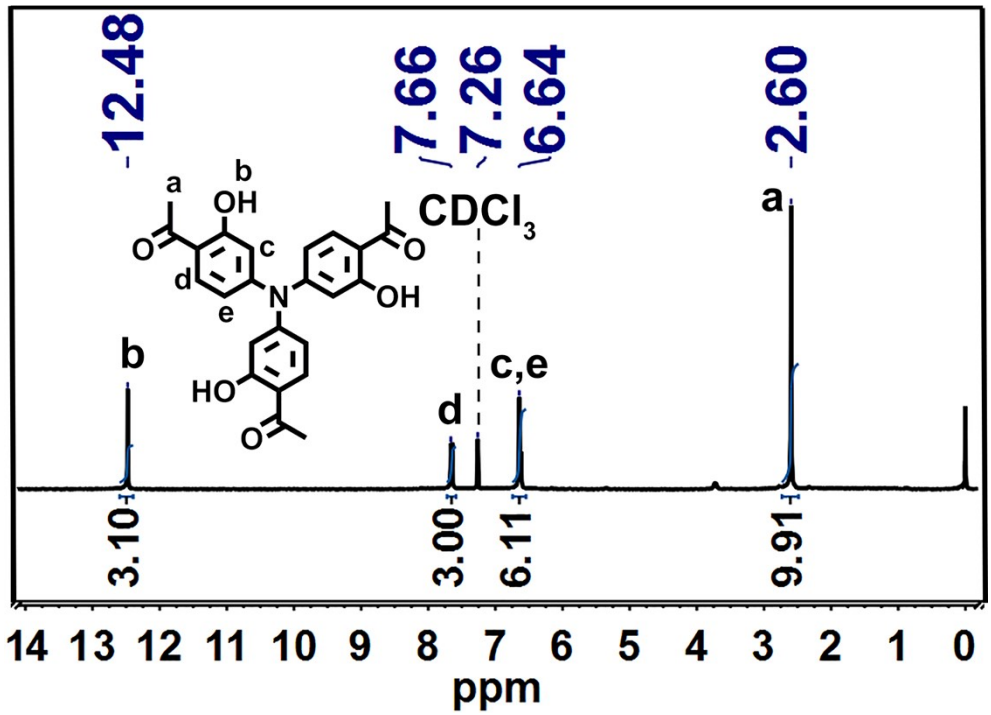

Figure S5 400 MHz ^{1}H NMR spectrum of 3, 3', 3 "-trihydroxy-4, 4', 4" -triacetyl triphenylamine in $CDCl_3$.

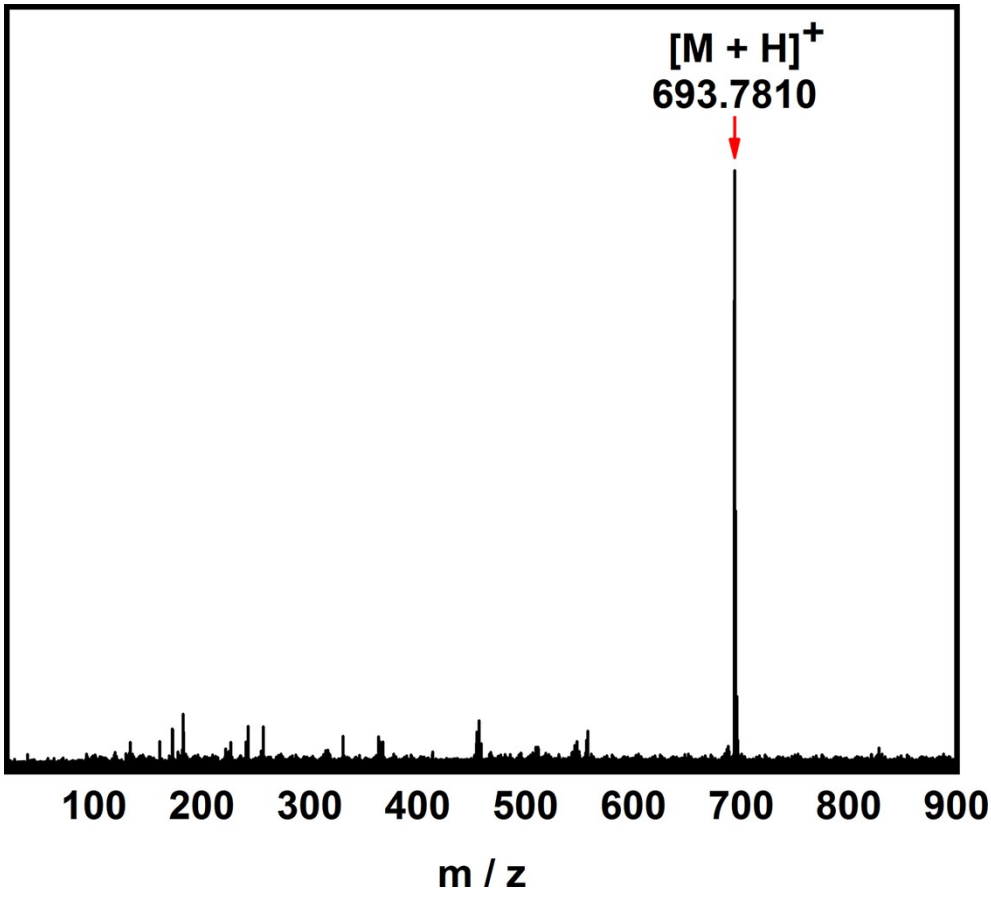

Figure S6 ESI-MS spectrum of tri (3- (2-) pyridyl methoxy) - tri (4- : acetyl) triphenylamine.

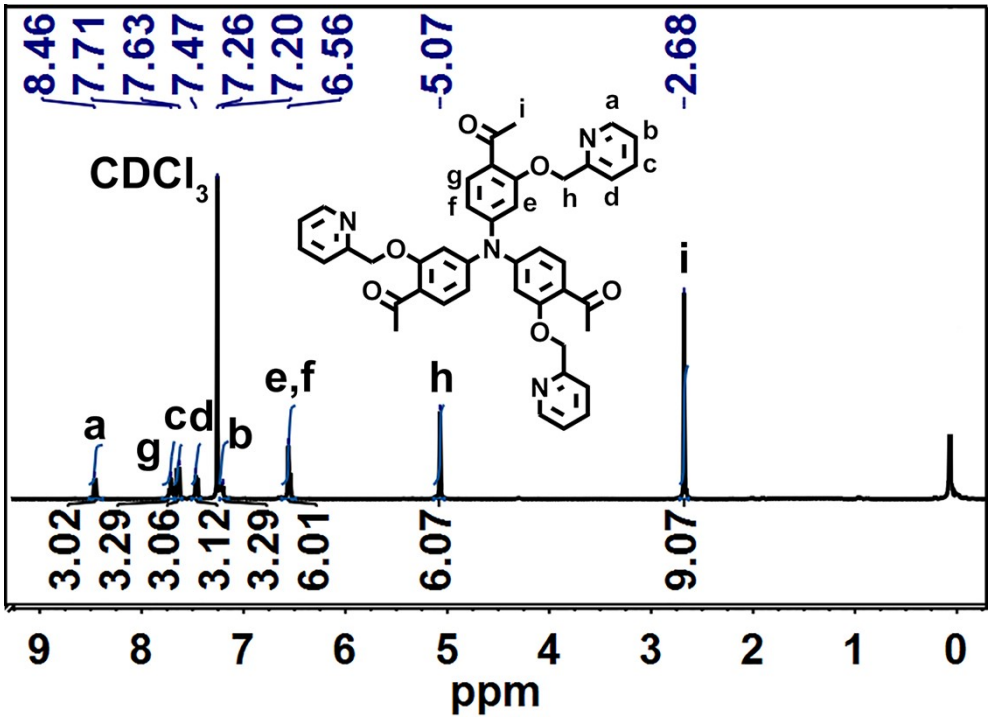

Figure S7 400 MHz ^{1}H NMR spectrum of tri (3- (2-) pyridyl methoxy) - tri (4- : acetyl) triphenylamine in $CDCl_3$.

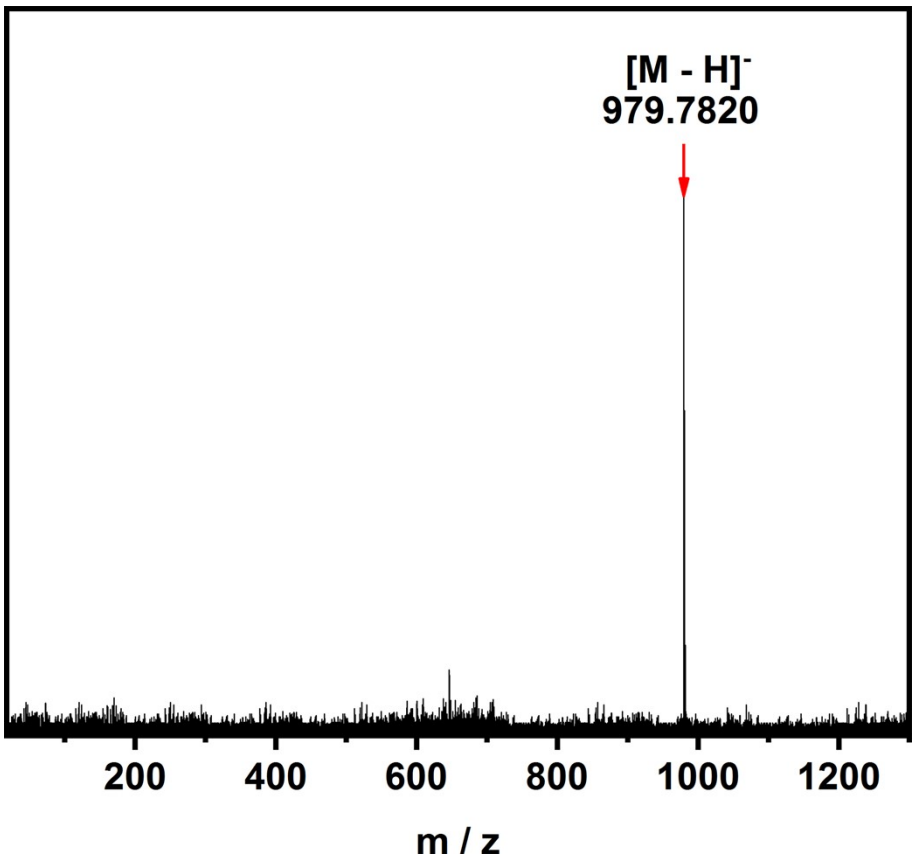

Figure S8 ESI-MS spectrum of ligand **L[4]**.

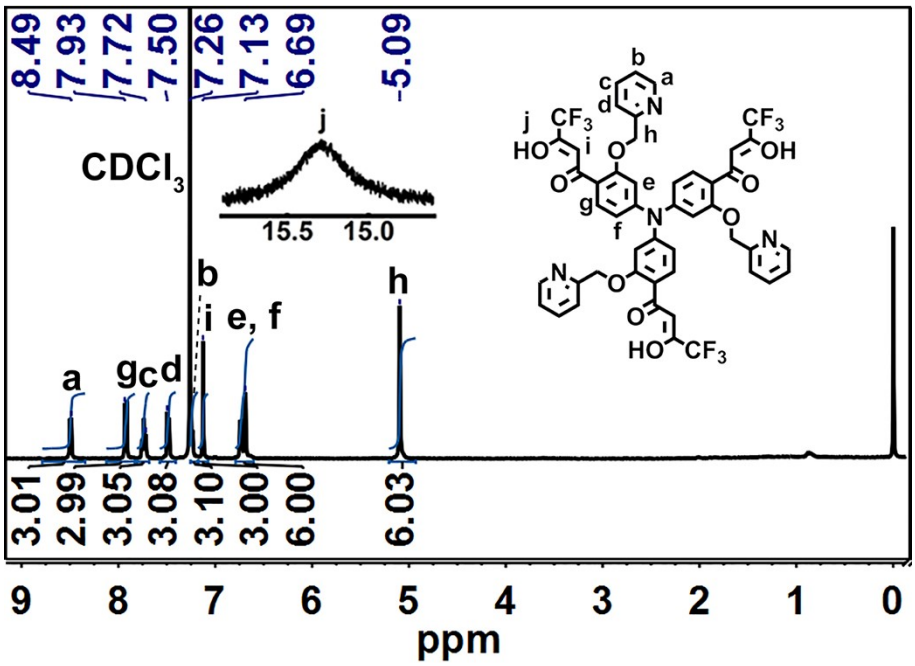

Figure S9 400 MHz ^{1}H NMR spectrum of ligand **L[4]** in $CDCl_3$.

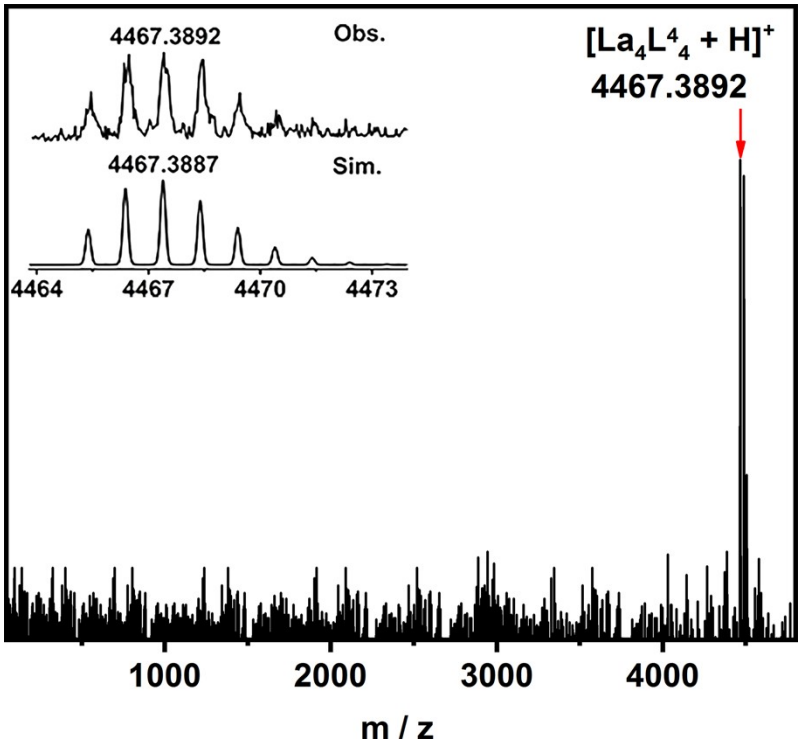

Figure S10 ESI-TOF-MS of tetrahedra $La_4\mathbf{L}^4_4$ with insets showing the observed (Obs.) and simulated (Sim.) isotopic patterns of the cation $[La_4\mathbf{L}^4_4 + H]^+$ peaks.

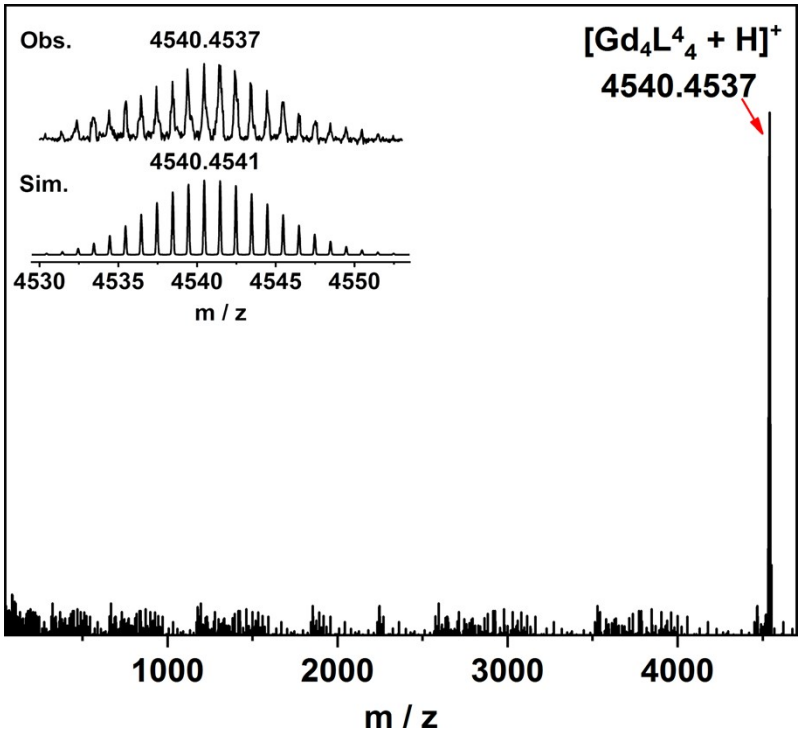

Figure S11 ESI-TOF-MS of tetrahedra $Gd_4\mathbf{L}^4_4$ with insets showing the observed (Obs.) and simulated (Sim.) isotopic patterns of the cation $[Gd_4\mathbf{L}^4_4 + H]^+$ peaks.

2.1 Sensing experiments.

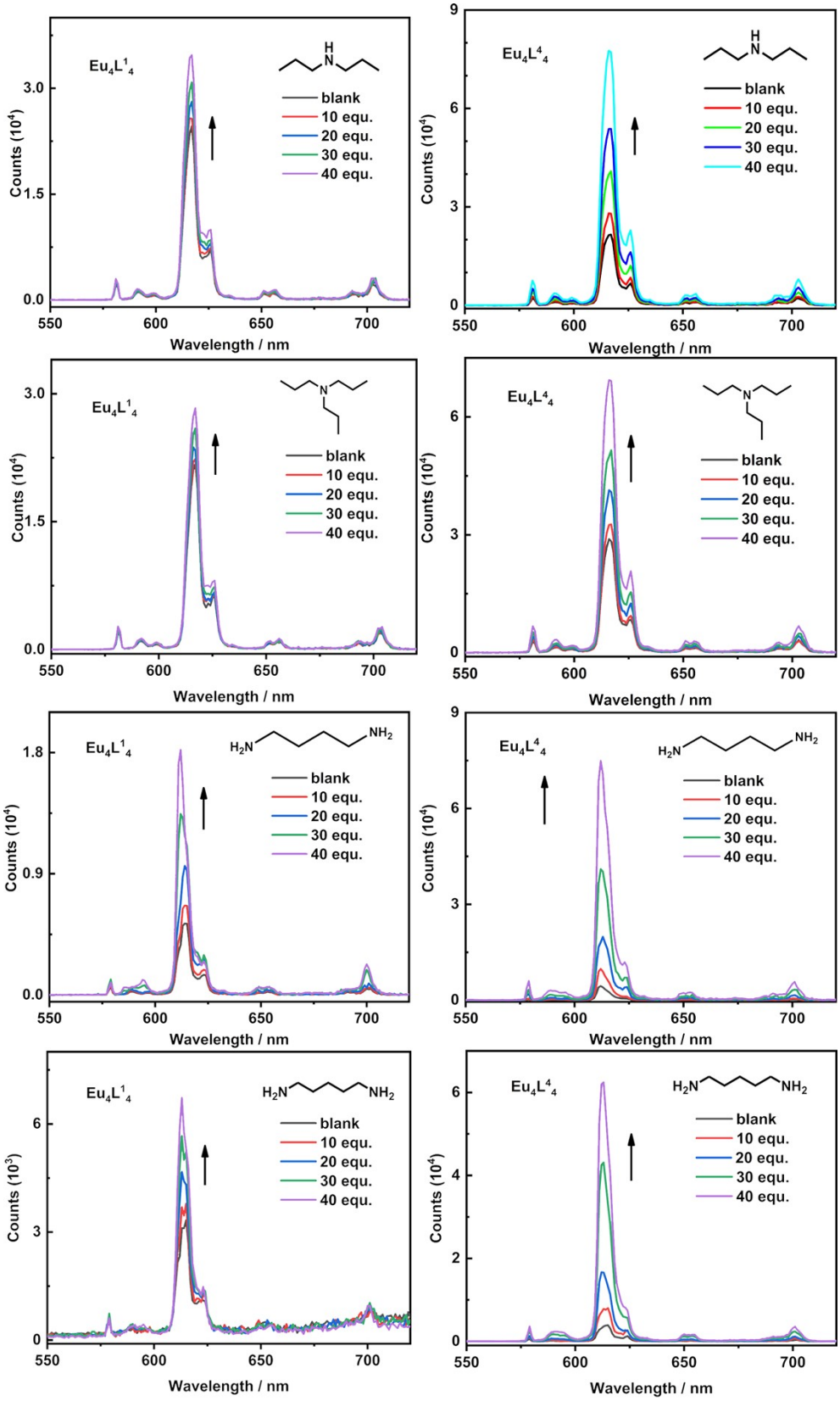

Figure S12 Emission spectra of $Eu_4\mathbf{L^1}_4$ and $Eu_4\mathbf{L^4}_4$ upon the addition of different concentration of amines (λ_{ex} = 390 nm).

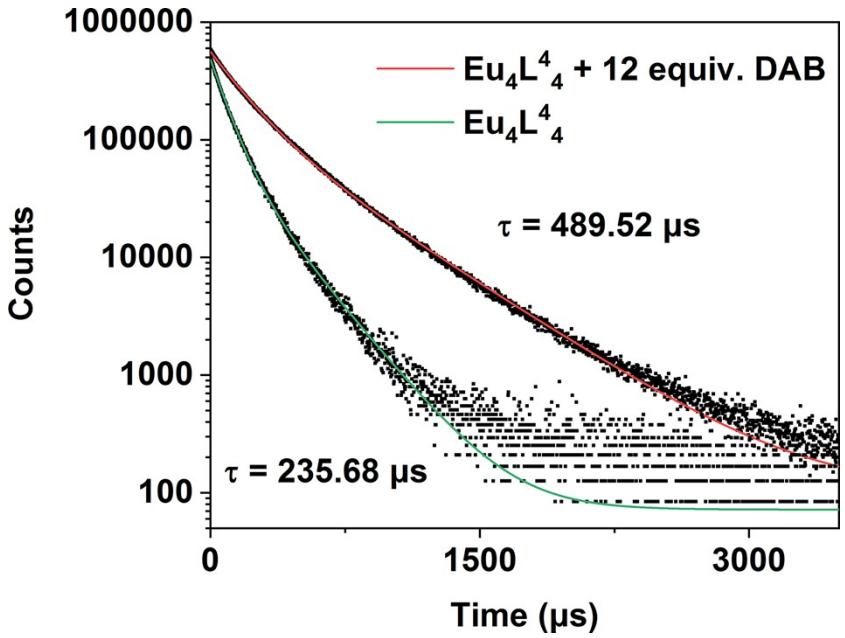

Figure S13 Lifetime of $Eu_4L^4_4$ with adding DAB in THF. (c=0.25 x 10^{-5}M).

2.2 Calculation of detection limit (LoD)

The detection limits of $Eu_4L^4_4$ were determined by 3σ/S. In the first step, the backgroud noise of $Eu_4L^4_4$ was determined by calculating the standard deviation of the emission intensity in the N data points recorded before amine exposure. The detection limits was then calculated following Eq. 3, where *slope* is the slope of the linear regression fit of the $Eu_4L^4_4$ response vs. amines concentration (See Figure S14).

$$noise = \sigma = \sqrt{\frac{1}{N}\sum_{i=1}^{N}(\mu - x_i)^2} \qquad (1)$$

$$\mu = \frac{1}{N}(x_1 + \ldots + x_n) \qquad (2)$$

$$LoD = 3\frac{noise}{slope} \qquad (3)$$

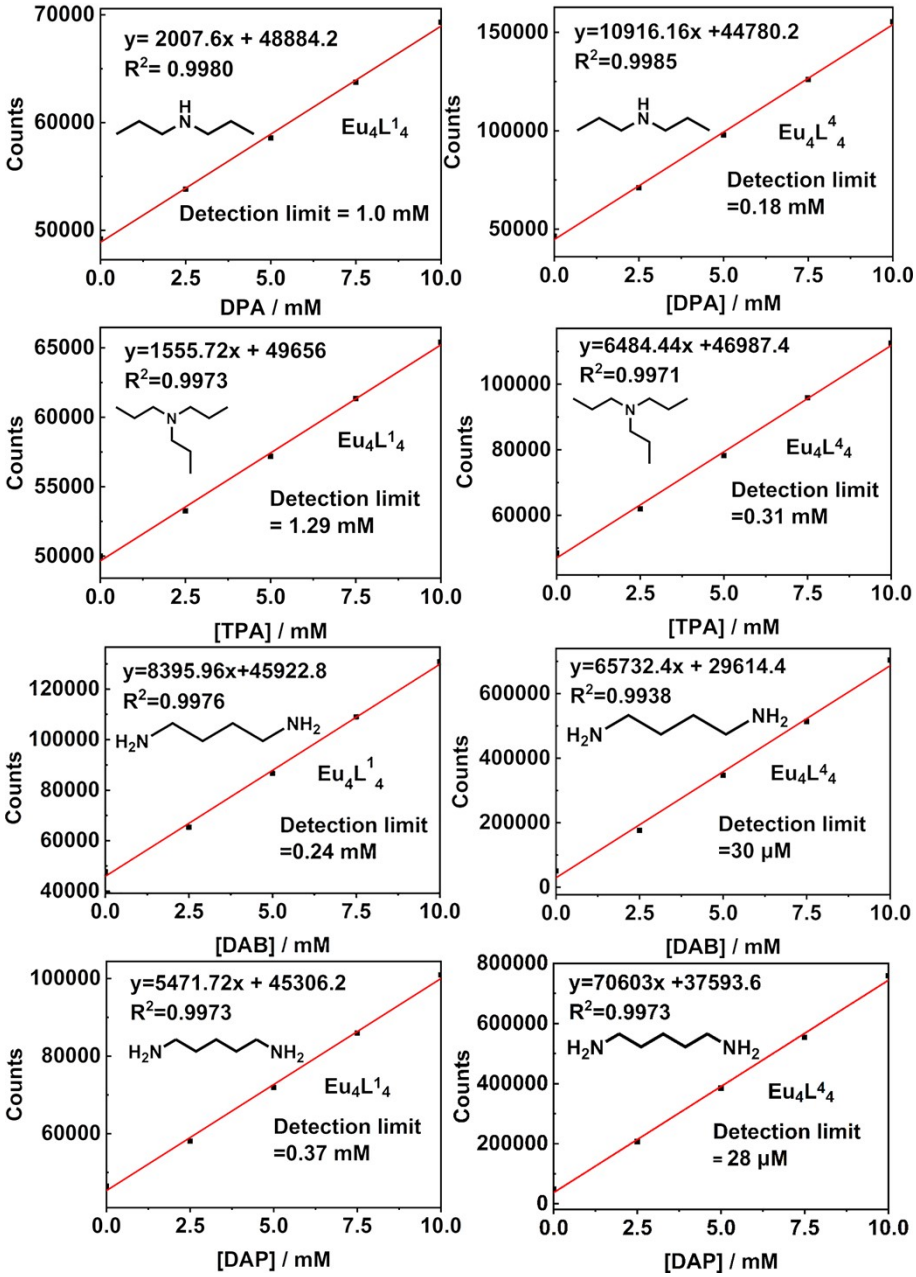

Figure S14 Linear range of luminescence response for $Eu_4\mathbf{L^1}_4$ and $Eu_4\mathbf{L^4}_4$ towards different concentration of amine. The slopes of the linear regressions were used in calculating the detection limt of the corresponding amines.

Table S1 The detection limits of $Eu_4\mathbf{L^4}_4$ for a series of biogenic amines.

	EDA	DAB	DAP	PA	DPA	TPA
Detection limit (mM)	0.033	0.03	0.028	0.22	0.18	0.31

Table S2 The detection limits of $Eu_4L^1_4$ for a series of biogenic amines.

	EDA	DAB	DAP	PA	DPA	TPA
Detection limit (mM)	0.39	0.24	0.37	1.12	1.0	1.29

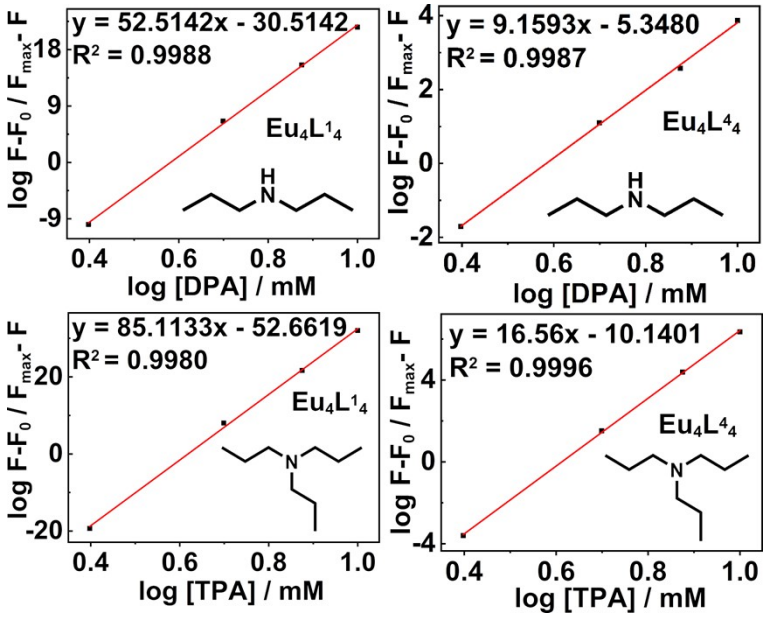

Figure S15 Linear range of log $F\text{-}F_0$ / F_{max} -F for $Eu_4L^1_4$ and $Eu_4L^4_4$ towards log[monamine]. The reciprocal of the intercept of the linear regressions were binding constant of $Eu_4L^1_4$ and $Eu_4L^4_4$. (F_0: the initial luminescence intensity; F: the luminescence intensity after adding different concentration of monamine; F_{max}: The luminescence intensity at saturation binding).

Table S3 The binding constant of $Eu_4L^1_4$ and $Eu_4L^4_4$ for a series of monamine.

Binding constant (10^3) M^{-1}	PA	DPA	TPA
$Eu_4L^1_4$	0.04968	0.03277	0.01899
$Eu_4L^4_4$	0.2820	0.1870	0.09860

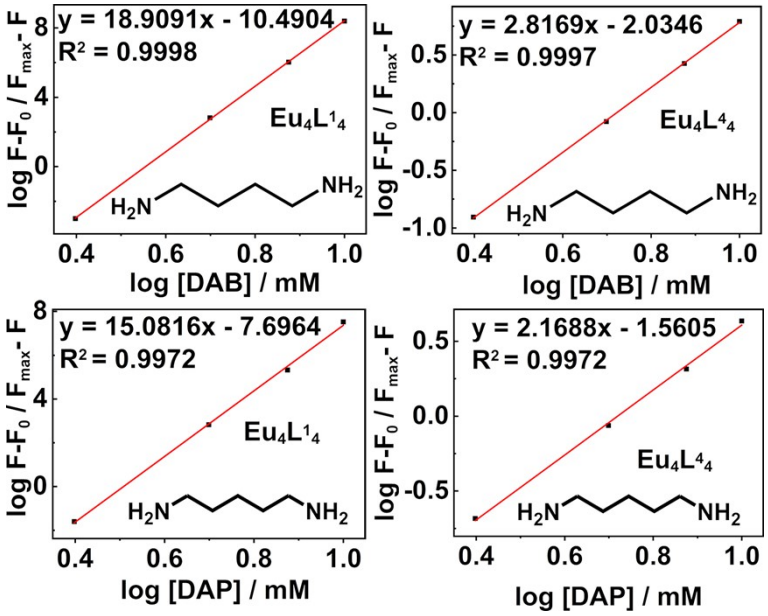

Figure S16 Linear range of log F-F_0 / F_{max} -F for $Eu_4\mathbf{L^1}_4$ and $Eu_4\mathbf{L^4}_4$ towards log[diamine]. The reciprocal of the intercept of the linear regressions were binding constant of $Eu_4\mathbf{L^1}_4$ and $Eu_4\mathbf{L^4}_4$. (F_0: the initial luminescence intensity; F: the luminescence intensity after adding different concentration of diamine; F_{max}: The luminescence intensity at saturation binding).

Table S4 The binding constant of $Eu_4\mathbf{L^1}_4$ and $Eu_4\mathbf{L^4}_4$ for a series of diamine.

Binding constant (10^3) M^{-1}	EDA	DAB	DAP
$Eu_4\mathbf{L^1}_4$	0.07447	0.09533	0.1299
$Eu_4\mathbf{L^4}_4$	0.4229	0.4915	0.6408

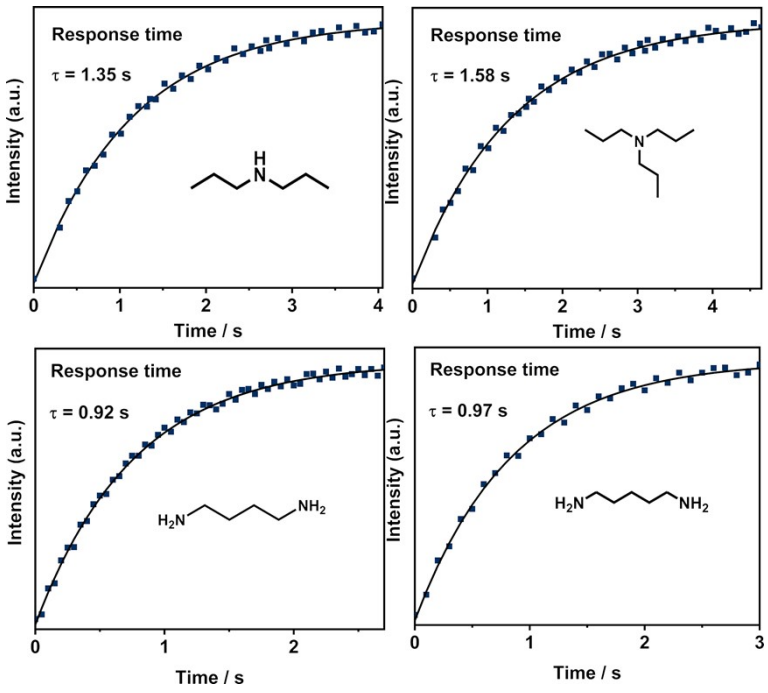

Figure S17 Time-resolved emission intensity of $Eu_4\mathbf{L^4}_4$ upon adding biogenic amines.

Table S5 Summary of fluorescence sensing properties of various sensors 1–34 for BAs and NH_3

Sensor	Sensing analyte	Selectivity	LOD	Response time	Reversibility	Reference
1	BAs	good	-	< 1 s	Reversible	1
2	BAs/NH_3	-	-	1 min	Reversible	2
3	BAs	good	0.15 μm	< 1 min	-	3
4	BAs	good	62.1 nM	< 1 min	Irreversible	4
5	BAs	good	2.53 nM	>200 s	-	5
6	BAs	good	209 nM	40 min	-	6
7	BAs / NH_3	good	6.9 nM 62 nM	< 5 min	-	7
8	BAs (amine vapor)	good	3.82 ppm	1 min	-	8
9	BAs amine vapor	good	46 nM 8.65 ppm	15 s	-	9
10	BAs	good	14 nM	60 s	-	10
11	BAs / amine vapor	good	180 to 400 nM for diamines 4.3 ppm for putrescine	-	Irreversible	11
12	Amine / NH_3	good	6.85 ppm	-	-	12
13	Amine vapors	good	12.7 ppm	-	-	13
14	Amine vapors	good	8.4 ppm	-	-	14
15	Amine vapors	good	690 ppb for NH_3	-	-	15
16	NH_3	good	-	87 s	Reversible	16
17	NH_3	-	-	3-15 s	Reversible	17
18	NH_3	good	6.5 ppb (384 nM)	-	Reversible	18
19	NH_3	good	5 ppm	< 5 s	Reversible	19
20	NH_3	-	5.8925×10^{-4}	< 1 s	Reversible	20
21	Organic amines	good	0.35 μM, 2.22 μM, and 1.26 μM	-	-	21
22	Amine vapors	good	80 ppm	< 20 s	-	22
23	Organic amines	good	sub-ppm	-	Reversible	23
24	Organic amines	good	-	-	-	24
25	Methylaminevapors	-	-	-	Reversible	25
26	Organic amine vapors	good	-	-	-	26
27	Histidine	good	0.18 μM	1 min	-	27
28	BAs	good	-	112 ms	Reversible	28
29	BAs	good	13.9 ppm	73 ms	Reversible	29
30	BAs	good	1.83 ppm	< 2 s	-	30
31	BAs	good	0.41 mu mol/L-1.14 mu mol/L	2-8 s	- -	31
32	4.3 ppb and 5.1 ppb for spermine and spermidine	good	4.3 ppb and 5.1 ppb for spermine and spermidine	-	-	32
33	BAs	good	$12.8\text{-}13.4 \times 10^{-8}$ M	28s	-	33
34	spermine and spermidine	good	15.29 nM (3.07 ppb) and 10.29 nM (2.08 ppb)	< 5 s	-	34

Reference

[1] R. Jia, W. Tian, H. Bai, J. Zhang, S. Wang and J. Zhang, Nature Commun., 2019, 10, 795.

[2] Y. Liu, Y. Xiao, M. Shang, Y. Zhuang and L. Wang, Chem Eng J. 2022;428, 132647.

[3] L. Wang, H. Ding, H. Tang, D. Cao, X. Ran, Analytica Chimica Acta, 2020, 1135, 38−46.

[4] L. Wang, S. Xin, C. Zhang, X. Ran, H. Tang and D. Cao, J. Mater. Chem. B, 2021, 9, 9383–9394.

[5] L. Li, W. Li, X. Ran, L. Wang, H. Tang and D. Cao, Chem. Commun., 2019, 55, 9789–9792.

[6] B. Zhu, L. Jiang, T. Chen, G. Bao, L. Zeng, X. Hu, H. Yuan, Dyes and Pigments, 2021, 186, 108963.

[7] S. Jeon, T. Kim, H. Jin, U. Lee, J. Bae, J. Bouffard and Y. Kim, J. Am. Chem. Soc., 2020, 142, 9231−9239.

[8] Y. Meng, C. Yuan, C. Du, K. Jia, C. Liu, K. Wang, S. Chen, Z. Hu, Spectrochimica Acta Part A: Molecular and Biomolecular Spectroscopy, 2021, 262, 120152.

[9] L. Jiang, H. Ye, D. Ma, J. Rodrigues, R. Sheng and D. Min, Analyst, 2022, 147, 923–931.

[10] H. Ye, S. Koo, B. Zhu, Y. Ke, R. Sheng, T. Duan, L. Zeng, J. S. Kim, Anal. Chem., 2022, 94, 15423−15432.

[11] R. Roy, N. R. Sajeev, V. Sharma and A. L. Koner, ACS Appl Mater Interfaces, 2019, 11, 47207−47217.

[12] E. Zhang, X. Hou, H. Yang, Y. Zou and P. Ju, Anal. Methods, 2020, 12, 1744–1751.

[13] C. Bao, S. Shao, H. Zhou and Y. Han, New J. Chem., 2021, 45, 10735–10740.

[14] M. Gao, S. Li, Y. Lin, Y. Geng, X. Ling, L. Wang, A. Qin and B. Tang, ACS Sens., 2016, 1, 179−184.

[15] P. Alam, N. L. C. Leung, H. Su, Z. Qiu, R. T. K. Kwok, J. W. Y. Lam and B. Tang, Chem. Eur. J., 2017, 23, 14911–14917.

[16] Y. Li, S. Li, Y. Jiang, M. Hu and Q. Zhai, Chem. Commun., 2018, 54, 9789−9792.

[17] B. Zhu, Y. Jin, J. Chu, M. Zuo and S. Cui, RSC Adv., 2022, 12, 6951–6957.

[18] D. I. Pavlov, T. S. Sukhikh, A. A. Ryadun, V. V. Matveevskaya, K. A. Kovalenko, E. Benassi, V. P. Fedin and A. S. Potapov, J. Mater. Chem. C, 2022, 10, 5567–5575.

[19] Y. Cheng, Q. Feng, M. Yin, C. Wang, Y. Zhou, Tetrahedron Lett., 2016, 57, 3814–3818.

[20] N. Xu, R. Wang, D. Li, Z. Zhou, T. Zhang, Y. Xie and Z. Su, New J. Chem., 2018, 42, 13367–13374.

[21] I. Ahmed, H. J. Lee, S. H. Jhung, J. Mol. Liq., 2021, 344, 117765.

[22] P. Li, Z. Li, D. Yao and H. Li, J. Mater. Chem. C, 2017, 5, 6805–6811.

[23] D. Gu, W. Yang, D. Lin, X. Qin, Y. Yang, F. Wang, Q. Pan and Z. Su, J. Mater. Chem. C, 2020, 8, 13648–13654.

[24] Y. Li, T. Wang, D. Yang, Y. Wang and H. Li, New J. Chem., 2017, 41, 14103–14108.

[25] N. V. Petrochenkova, A. G. Mirochnik, T. B. Emelina, A. A. Sergeev, A. A. Leonov, S. S. Voznesenskii, Spectrochimica Acta Part A: Molecular and Biomolecular Spectroscopy, 2018, 200, 70–75.

[26] X. Shen and B. Yan, J. Mater. Chem. C, 2015, 3, 7038–7044.

[27] L. Song, J. Xiao, R. Cui, X. Wang, F. Tian, Z. Liu, Sensors and Actuators: B. Chemical, 2021, 336, 129753.

[28] Y. Yao, J. Li, Y. Zhou, T. Gao, H. Li, P. Yan. Turn-on luminescence detection of biogenic amine with an Eu(III) tetrahedron cage. Dyes and Pigments, 2021, 192, 109441.

[29] Y. Yao, C. Zhao, Y. Zhang, G. Cai, F. Wu, J. Sun, X. Liu, T. Zhou, S. Wang, L. Jiang, M. Chen, S. Wang, N. Wu, G. Liu, H. Li. Real time NIR detection of biogenic amine using an Yb_4L_4 tetrahedron. Optical Materials, 2024, 147, 114790.

[30] X. Zhao, W. Wang, J. Cheng, Y. Xia, C. Duan, R. Zhong, X. Zhao, X. Li, Y. Ni. Nanolignin-containing cellulose nanofibrils (LCNF)-enabled multifunctional ratiometric fluorescent bio-nanocomposite films for food freshness monitoring. 2024, 453, 139673.

[31] H. Chen, X. Dong, K. Ou, X. Cong, Y. Liao, Y. Yang, H. Wang. A pH-responsive dual-emission composite for fast detection of BAs and visual monitoring seafood freshness with large luminescence color difference. Talanta, 2025, 282, 126946.

[32] A. Thakuri, R. Acharya, M. Banerjee, A. Chatterjee. A polydiacetylene (PDA) based dual-mode optical sensor for the ppb level selective detection of biogenic polyamines. Sensors and Actuators B: Chemical, 2024, 409, 135573.

[33] D. Bariya, S. Mishra. Fluorescent-based bile acid triazole-phenothiazine derivatives: Multiphase detection of biogenic amines and application in spoiled foods. Microchemical Journal, 2024, 207, 111707.

[34] S. K. Pandit, G. Das. Fluorescence detection of spermine and spermidine using a poly-carboxylate receptor and ensemble-based formalin sensing in real samples. New J. Chem., 2025, 49, 3930.

Table S6 The intensity ratio of the $^5D_0 \rightarrow {}^7F_2$ to $^5D_0 \rightarrow {}^7F_1$ transitions (I_{7F2}/I_{7F1}) of $Eu_4\mathbf{L^4_4}$ for EDA.

Equiv. of added EDA		0	10 equiv.	20 equiv.	30 equiv.	40 equiv.
Counts (10^4)	$7F_2$	0.046	1.00	1.97	3.88	6.43
	$7F_1$	0.023	0.051	0.094	0.19	0.32
I_{7F2}/I_{7F1}		20.00	19.61	20.95	20.26	20.09

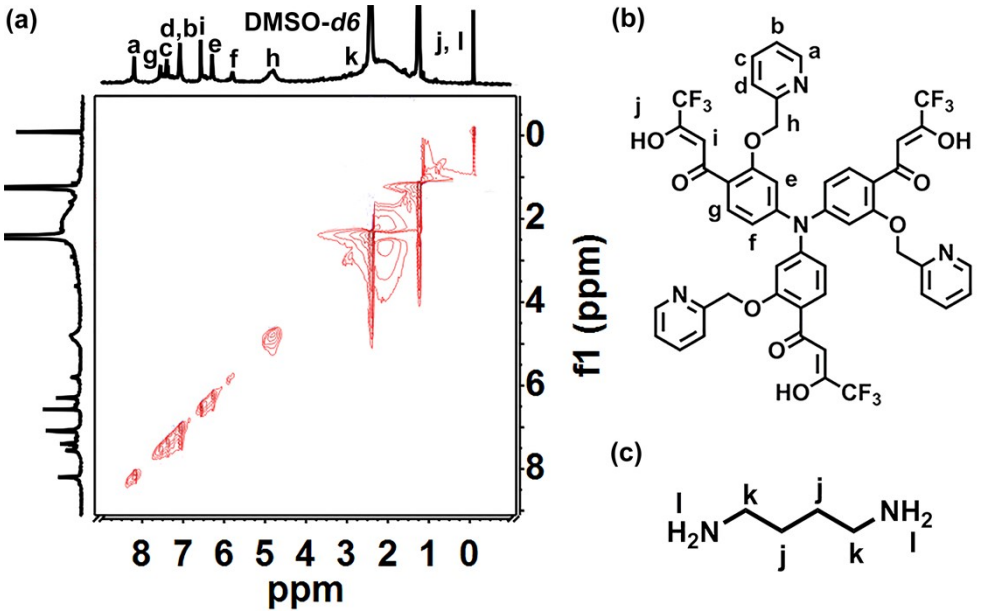

Figure S18 NOESY (400 MHz) spectrum of $La_4\mathbf{L^4_4}$ with adding DAB in DMSO-*d6*. (a) NOESY of $La_4\mathbf{L^4_4}$ with adding DAB. (b) NMR assignment of $\mathbf{L^4}$. (c) NMR assignment of DAB.

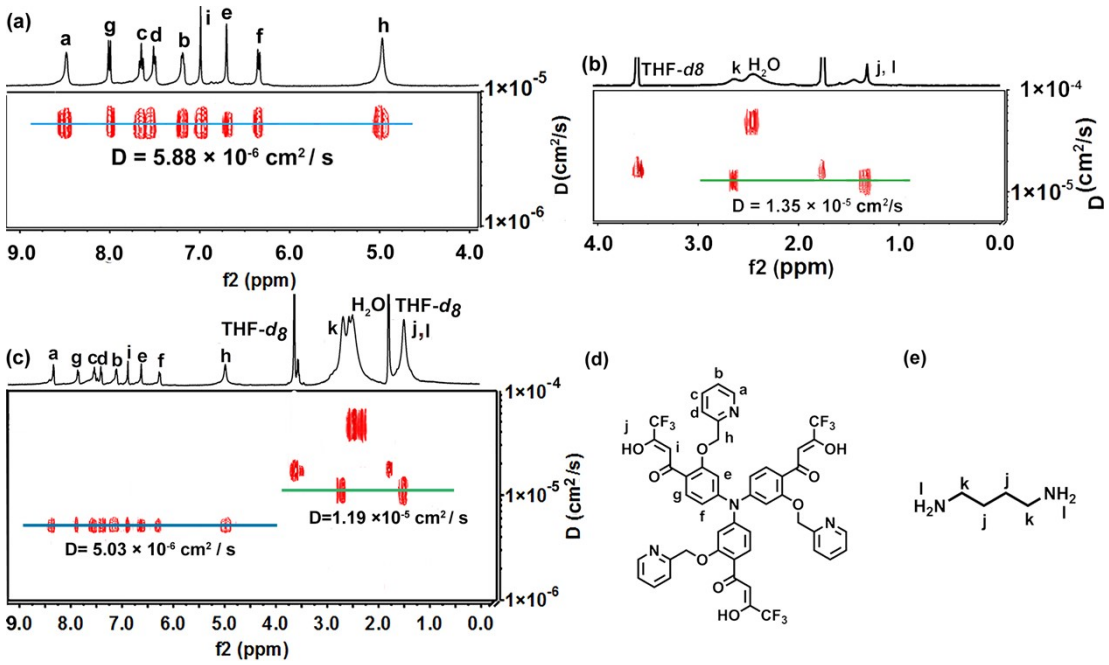

Figure S19 2D-1H-DOSY NMR spectra of $La_4\mathbf{L^4_4}$ with adding DAB in THF-*d8*. (a) DOSY of $La_4\mathbf{L^4_4}$. (b) DOSY of DAB. (c) DOSY of $La_4\mathbf{L^4_4}$ with adding DAB. (d) NMR assignment of $\mathbf{L^4}$. (e) NMR assignment of DAB.

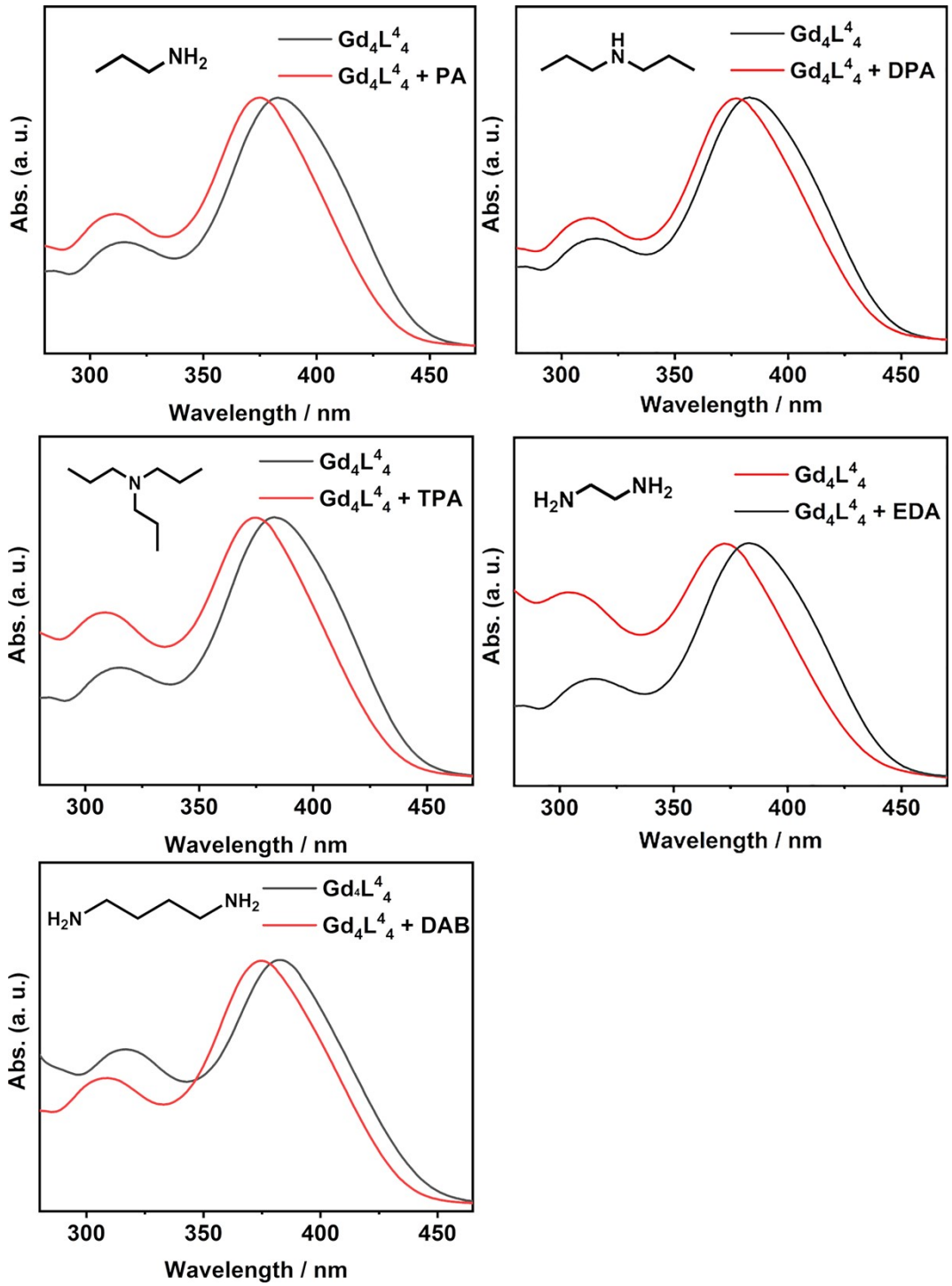

Figure S20 UV/vis absorption spectral changes of $Gd_4\mathbf{L}^4{}_4$ by the addition of various amines in THF/CH_3CN. (v_{THF}/v_{CH3CN}= 1:9, 0.25 × 10^{-5} M).

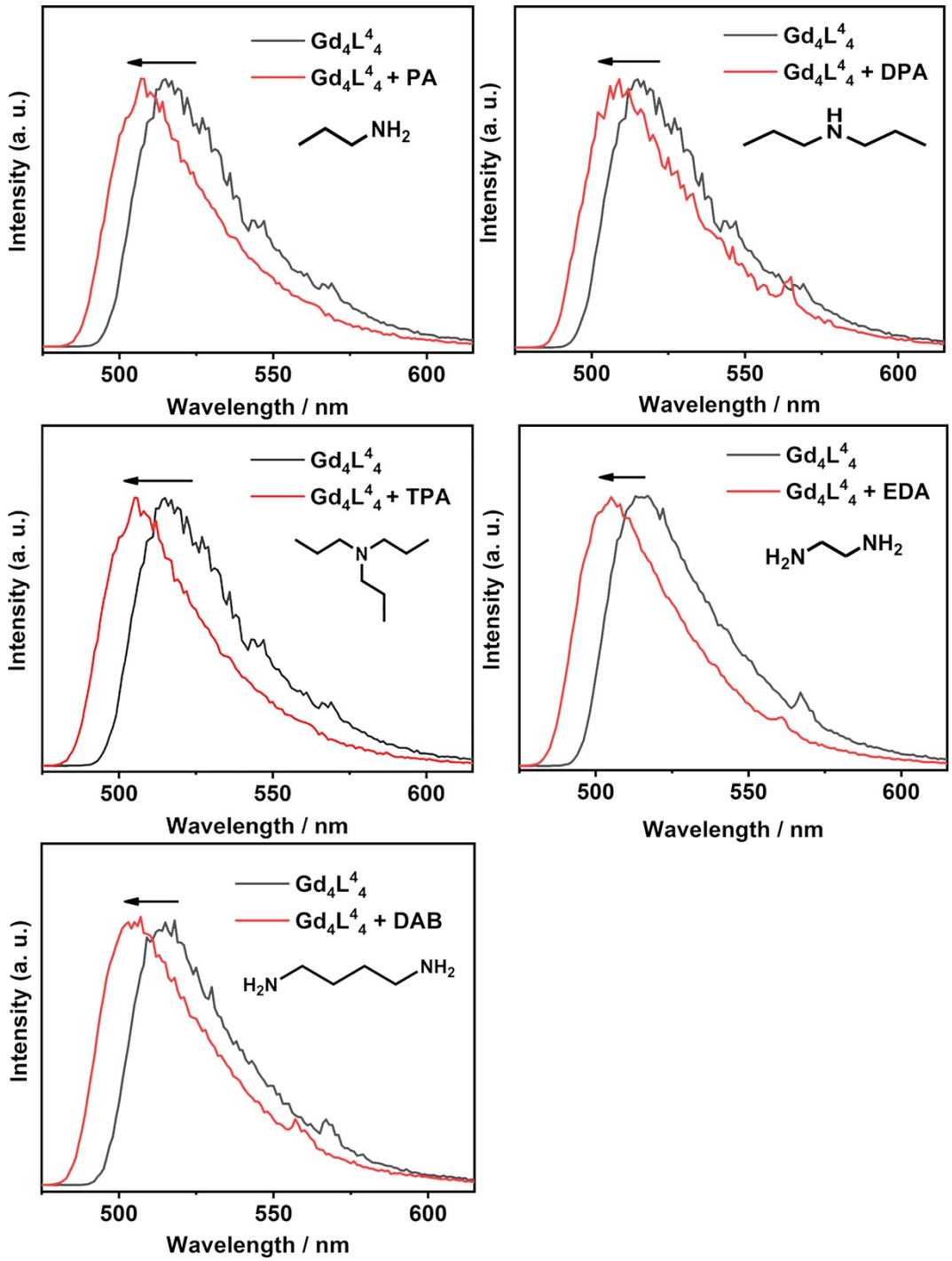

Figure S21 Phosphorescence emission spectral changes of $Gd_4L^4{}_4$ by the addition of various amines in THF/CH_3CN. (v_{THF}/v_{CH3CN}= 1:9, 0.25 × 10^{-5} M).